ELSEVIER

Nuclear Instruments and Methods in Physics Research A 406 (1998) 411–426

NUCLEAR INSTRUMENTS & METHODS IN PHYSICS RESEARCH Section A

A large-scale low-background liquid scintillation detector: the counting test facility at Gran Sasso

G. Alimonti[a], C. Arpesella[c], G. Bacchiocchi[a], M. Balata[c], G. Bellini[a], J. Benziger[d,*], S. Bonetti[a], A. Brigatti[a], L. Cadonati[e], F.P. Calaprice[e], R. Cavaletti[a], G. Cecchet[f], M. Chen[e], N. Darnton[e], A. deBari[f], M. Deutsch[g], F. Elisei[h], F. von Feilitzsch[b], C. Galbiati[a], A. Garagiola[a], F. Gatti[i], M.G. Giammarchi[a], d. Giugni[a], T. Goldbrunner[b], A. Golubchikov[j], A. Goretti[a], S. Grabar[a], T. Hagner[b], F. Hartmann[a], R. von Hentig[b], G. Heusser[k], A. Ianni[a], J. Jochum[b], M. Johnson[d], M. Laubenstein[c], F. Loeser[e], P. Lombardi[a], S. Magni[a], S. Malvezzi[a], I. Manno[a], G. Manuzio[i], F. Masetti[h], U. Mazzucato[h], E. Meroni[a], M. Neff[b], S. Nisi[c], A. Nostro[i], L. Oberauer[b], A. Perotti[f], A. Preda[a], P. Raghavan[l], R.S. Raghavan[l], G. Ranucci[a], E. Resconi[a], P. Ruscitti[i], R. Scardaoni[a], S. Schoenert[b], O. Smirnov[j], R. Tartaglia[c], G. Testera[i], P. Ullucci[a], R.B. Vogelaar[e], S. Vitale[i], O. Zaimidoroga[j]

[a] *Physics Dept. of the University and INFN, Milano, Italy*
[b] *Technical University Munich, Garching, Germany*
[c] *Laboratori Nazionali del Gran Sasso, Assergi (Aq), Italy*
[d] *School of Engineering, Princeton University, Princeton, NJ, USA*
[e] *Physics Department, Princeton University, Princeton, NJ, USA*
[f] *Physics Department of the University and INFN, Pavia, Italy*
[g] *Massachusetts Institute of Technology, Cambridge, MA, USA*
[h] *Physics Department of the University and INFN, Perugia, Italy*
[i] *Physics Department of the University and INFN, Genova, Italy*
[j] *Joint Inst. For Nuclear Research, Dubna, Russia*
[k] *Max-Planck-Institute, Heidelberg, Germany*
[l] *Lucent Technologies, Murray Hill, NJ, USA*

Received 11 August 1997; received in revised form 23 September 1997

Abstract

A 4.8 m^3 unsegmented liquid scintillation detector at the underground Laboratori Nazionali del Gran Sasso has shown the feasibility of multi-ton low-background detectors operating to energies as low as 250 keV. Detector construction and the handling of large volumes of liquid scintillator to minimize the background are described. The scintillator, 1.5 g PPO/L-pseudocumene, is held in a flexible nylon vessel shielded by 1000 t of purified water. The active detector volume is viewed by 100 photomultipliers, which measure time and charge for each event, from which energy,

* Corresponding author. Tel.: + 1 609 258 5416; fax: + 1 609 258 0211; e-mail: benziger@princeton.edu.

0168-9002/98/$19.00
PII S0168-9002(98)00018-7

position and pulse shape are deduced. On-line purification of the scintillator by water extraction, vacuum distillation and nitrogen stripping removed radioactive impurities. Upper limits were established of $< 10^{-7}$ Bq/kg-scintillator for events with energies 250 keV $< E <$ 800 keV, and $< 10^{-9}$ Bq/kg-scintillator due to the decay products of uranium and thorium. The isotopic abundance of $^{14}C/^{12}C$ in the scintillator was shown to be approximately 10^{-18} by extending the energy window of the detector to 25–250 keV. The ^{14}C abundance and uranium and thorium levels in the CTF are compatible with the Borexino Solar Neutrino Experiment.

1. Introduction

Large-scale (>100 t), low background (<1 event/day/t) underground particle detectors have acquired importance in the study of rare events, such as those associated with solar and atmospheric neutrino detection and stellar collapse [1–6], or the search for exotic phenomena such as dark matter [7,8], proton decay [9], and magnetic monopoles [10]. The sensitivity of these experiments is ultimately limited by the detector volume (which sets the signal rate) and the detector background. Although the magnitude and nature of this background varies among experiments, depending on the event signature, there are generally three main contributions:

1. Primary and secondary cosmic radiation. This background is reduced dramatically by locating the experiment underground. Further reduction is possible when the characteristics of the cosmic ray source may be identified.
2. Radiation from radioactivity in the laboratory environment and external detector components. Gamma rays and neutrons from sources external to the active detector volume may be absorbed by successive layers of shielding material, arranged as a "graded shield". The final shield usually consists of the outer region of the active detector, forming an "active" shield and defining an inner "fiducial volume".
3. Radioactive contamination from the active detector. The energy release from decay of long-lived nuclides is always below 5 MeV, the decay energy of ^{208}Tl (the "thallium barrier"). Detection of low-energy signals relies on both reducing radioactive impurities and/or identifying the signature of specific impurities and subtracting it from the background.

Almost without exception the detectors now in operation or under construction are either modular tracking arrays with scintillation counters (e.g. MACRO[11]) or water Cherenkov detectors (e.g. Kamioka[12] and SNO[13]). These detectors are limited to energies above the thallium barrier. Cherenkov detectors do not produce sufficient light below a few MeV energy, and modular scintillators contain too many radioactive contaminants. The only large, unsegmented underground scintillation detector described in the literature (Artemovsk [14]), also has too high a radioactive background to be useful at low energies.

This paper describes a moderately sized unsegmented liquid scintillation detector – the Counting Test Facility (CTF) – in the Underground Laboratory at Laboratori Nazionali del Gran Sasso. The scintillator is viewed by 100 photomultipliers immersed in 1000 t of purified water. The primary objective of the CTF was to determine the feasibility of a low background liquid-scintillation detector for signals with energies extending down to 250 keV, specifically for the Borexino Solar Neutrino Experiment [15]. The CTF detector was operated down to 25 keV to measure the ^{14}C β-spectrum with an endpoint of 156 keV. Borexino, which is now under construction, will detect the low-energy neutrinos from the decay of ^{7}Be in the sun by neutrino-electron scattering. The event signature is a sharp edge in the energy spectrum at the maximum recoil energy of 664 keV, well below the thallium barrier. The lack of an effectual event signature imposes severe limits on the tolerable background $\leqslant 10^{-9}$ Bq/kg in the energy range of the neutrino signal (250–800 keV).

Installation of the CTF began in 1993. The water shielding tank was filled in January of 1995, and the scintillator was introduced during February-April 1995. The CTF has operated almost continuously

until July 1997, when it was shut down for refurbishing and upgrading.

The CTF also provided tremendous insight into the construction and operation of a low background liquid scintillation detector, including:

- Radiopurity attainable in ton quantities of liquid scintillator.
- Clean handling procedures for large volumes of liquid scintillator.
- On-line scintillator purification.
- On-line purification of the shielding water.
- Radiopurity levels attainable for shielding materials.
- Materials selection and cleaning procedures for detector construction.
- Scintillator containment by a polymer membrane within a water buffer.
- Light propagation of scintillation light in a large volume 4π detector.
- Characterization of various types of events by the photoelectron time distribution, pulse height and shape.

Analysis of the data from the CTF suggested on-line purification of the scintillator reduced the intrinsic background in the energy window $250 < E < 800$ keV to the detection limit of the CTF. The relatively modest size of the CTF limits the extent of active shielding, setting a detection limit of 10^{-7} Bq/kg in the energy interval 250–800 keV. The limits for two of the most probable contaminants, radium and thorium, which have very distinct event signatures, were at a level of $\sim 10^{-9}$ Bq/kg. Between 25 and 250 keV the background is dominated by ^{14}C decay, with a rate of 0.1 mBq/kg, corresponding to an isotopic abundance of $^{14}C/^{12}C \sim 10^{-18}$.

This paper describes the overall design and operation of the Counting Test Facility. More detailed descriptions of the key elements of the detector are published elsewhere, including the scintillator containment system [16], the scintillator purification system [17], the shielding water purification system [18,19], the optical properties of the scintillator [20,21], the photomultipliers and data acquisition system [22–29] the optical concentrators [30] and the radon monitoring system [31]. Detailed reporting of the results obtained with the CTF [32] and for the ^{14}C concentration in the scintillator [33] are also published separately.

An overview of the CTF and its conceptual design is provided in Section 2. Section 3 provides a summary of the major components of the CTF detector. Section 4 describes the performance of the CTF, with a discussion of the functioning of the detector hardware. Finally, Section 5 highlights some of the key results obtained with the CTF concerning the background signals.

2. The counting test facility detector

The CTF serves as a calorimetric liquid scintillation detector. The scintillator is excited by decay of radioactive impurities contained within the scintillator, and by cosmogenic rays and γ-rays that pass through the detector. A schematic of the CTF detector, shown in Fig. 1, illustrates the shielding of the scintillator. The active detector is 4.8 m^3 of a binary liquid scintillator (1.5 g PPO/L pseudocumene). Scintillation light is detected with 100 phototubes surrounding the scintillator, and the arrival time and photon yield at each phototube are recorded.

The CTF detector is located in Hall C of the Gran Sasso underground laboratories, which provide 3500 m water-equivalent shielding from cosmic radiation. A muon flux of approximately 25/d/m^2 is the only residual cosmic radiation of consequence. Inside Hall C there is a γ-ray flux of approximately 10^8/d/m^2 from radioactive elements in the rocks. The active detector is 4.8 m^3 of an organic liquid scintillator immersed in 1000 t of pure water viewed by 100 photomultipliers. The water provides the equivalent of 4.5 m water shielding from the γ-rays on all sides. The phototubes contribute an additional γ-rays flux of approximately 2×10^6/d/m^2, and are moved 2.3 m away from the scintillator to permit the water to shield their γ-ray flux. Light collectors are affixed to the phototubes so they efficiently viewed the entire volume of the scintillator, providing 21% effective area coverage. The water is purified by deionization to minimize its contribution to background gamma radiation reaching the scintillator. Simulations suggest the water should reduce the external γ-ray

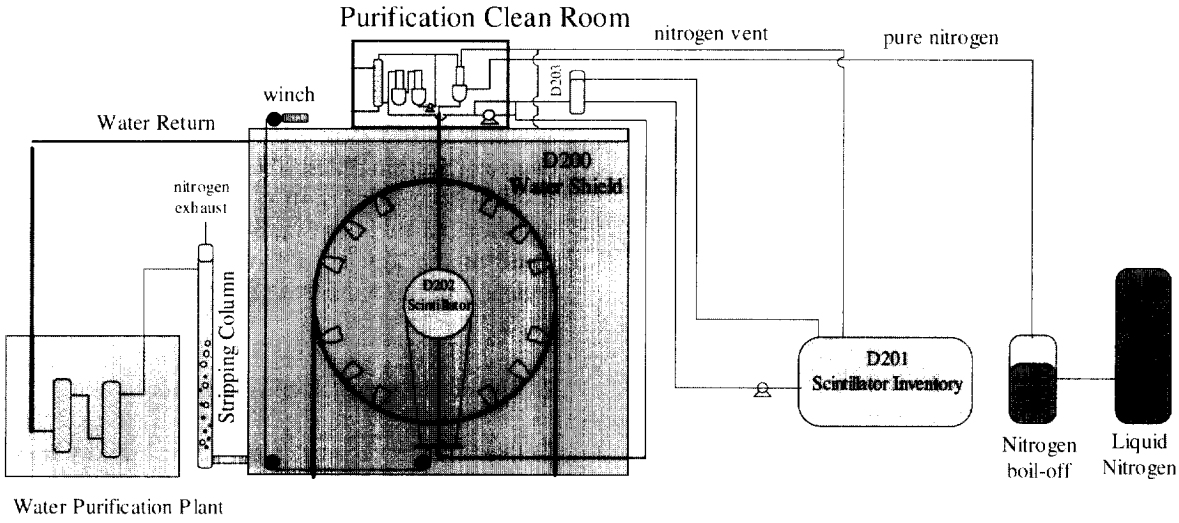

Fig. 1. Schematic of the counting test facility.

background from the rocks and phototubes to less than 100/d in the energy range 250–800 keV. U, Th and K concentrations in the shielding water at the level of 10^{-6} Bq/kg would contribute a background of 100/d; impurities in the water are expected to be the major source of background contributing between several hundred to a thousand scintillation events per day.

The internal background associated with the organic liquid scintillator is expected to be very low. Metal impurities, such as U, Th and K, typically exist as salts or oxides which are insoluble in nonpolar organic solvents used in the scintillator. In addition the principal components of the liquid scintillator are synthesized from petroleum which has resided deep in the earth for millions of years; as a result, most radioactive materials (e.g. ^{14}C) will have decayed away. Further improvement on the radiopurity of the liquid scintillator was accomplished through on-line purification.

Strict quality control was imposed over the materials of construction and the building techniques to avoid the introduction of unnecessary contamination. All the materials used in the CTF were tested for U, Th, Co, Cs, and K with high-sensitivity γ-ray spectroscopy, mass spectroscopy, or neutron activation. Assembly of the Counting Test Facility Detector was done under clean room conditions (nominal class 100 clean room) minimizing airborne contamination.

The PMTs and readout electronics allowed a refined measurement of arrival times and pulse shape discrimination, which facilitated the identification of the excitation source for events and their spatial reconstruction. Time correlation of events was employed to identify specific decay sequences associated with ^{85}Kr, ^{214}Bi–^{214}Po (used to infer the presence of Ra or Rn), and ^{212}Bi–^{212}Po (used to infer the presence of Th), and neutron interactions induced by cosmic muons. These analyses are discussed in greater detail elsewhere [33].

3. The CTF subsystems

The CTF detector integrates a variety of subsystems. Described below are the elements of the CTF detector, from the scintillator moving outward to the shielding and phototubes. The basic function of each of the major subsystems is described, along with special considerations for choice of materials and the method of preparation of the system.

3.1. The scintillator

Scintillator mixtures were evaluated for their optical properties, cost and availability, ease of purification, and chemical properties. The best compromise solution for the CTF was a two-component scintillator, consisting of 1.5 g PPO (2,5 diphenyl oxazole) per liter of pseudocumene (1,2,4 trimethylbenzene), PC. The density is 0.88 g/l at 15 C, and the refractive index is 1.5 at 420 nm.

The light yield from the scintillator and the decay times from excitation by γ-ray and α-particle excitation were obtained in laboratory samples [27,29]. The light yield of the PC-PPO scintillator was approximately 10^4 photons/MeV of energy deposited by fully relativistic particles such as β-rays and secondary electrons from γ-rays. For slower particles, the photon yield decreases [34,35]. The yield for 7.7 MeV α-particles from ^{214}Po decay is approximately 1000 photons/MeV. Scintillation from α-excitation was distinguished from β-excitation from the long time fluorescence tail [21,22,34,35].

Detailed studies of the absorption and fluorescence spectra of potential scintillator mixtures were carried out in the laboratory [20]. The maximum in the fluorescence spectrum of the chosen scintillator was at 365 nm, as measured in a conventional fluorescence spectrometer. The optical processes involved in the emission and propagation of scintillation light in a large detector are complex. At short wavelengths (<380 nm) the propagation is dominated by absorption of light (electronic state excitation) over short distances (<1 mm) followed by re-emission at longer wavelengths. Fluorescence light at longer wavelengths (>400 nm) cannot excite electronic transitions and the light is scattered by Rayleigh scattering, with a scattering length of the order of 10 m [36]. Simulations indicated that the light reaching the phototubes in the CTF has been red-shifted with a maximum around 400 nm. Absorption and reemission of light increases the apparent decay time from the scintillator from 3.5 ns. to 4.5–5 ns.

3.2. Scintillator containment vessel

The scintillator containment vessel confines the scintillator within the water buffer. Being in direct contact with water on the outside and scintillator on the inside, the vessel must be chemically compatible with both water and an aromatic solvent. The vessel sustains the 570 kg buoyant force associated with the 12% density difference between pesudocumene and water; it must be optically transparent to transmit the scintillation light, and it should not contribute significant background from radioimpurities.

These requirements were met by a flexible ball made of an amorphous nylon (Durethane C38F, Bayer Chemicals). The nylon obtained from Bayer was extruded into 0.5 mm thick sheets 1 m wide under controlled atmospheric conditions at Miles-Mobay (Pittsburgh, PA, USA). The nylon sheets were cut in an orange slice pattern and solvent welded over a spherical frame. Fabrication of the vessel was carried out at Princeton University in a class 100 clean room with the nylon sheets covered with Saran to minimize dust deposition. After fabrication the vessel was folded and shipped to Gran Sasso, were it was connected to the fluid-handling system inside the Main Tank and re-inflated.

Both the nylon sheets and the joints were tested to withstand 14 MPa stresses in water and pseudocumene before plastic deformation; the maximum design pressure in the CTF vessel was designed to be 3.5 MPa. In air, the 0.5 mm thick nylon has an optical transmittance of 80% at 365 nm; the remaining 20% of the light appears to be reflected and/or elastically scattered.

The scintillator containment vessel is a 1.05 m radius sphere. In the water buffer it is held in place by a system of 16 nylon strings attached to a movable plate via strain gauges. The hold down plate is moved by a winch and pulleys to accomodate stretching of the nylon strings resulting from the buoyant force. Both the buoyant force of the vessel and its position are monitored continuously to assure the shape and position of the vessel are maintained. Fig. 2 is a photo of the scintillator containment vessel inflated inside the CTF.

3.3. Scintillator handling

Filling and emptying of the scintillator containment vessel, circulating scintillator through a

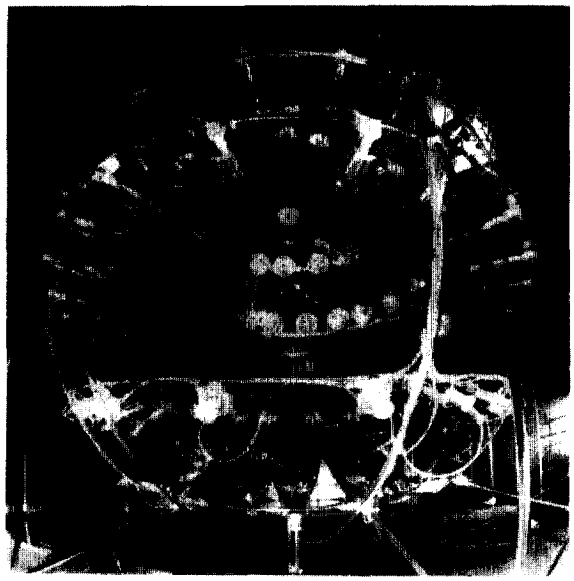

Fig. 2. Photo of the scintillator containment vessel inside the CTF.

purification system, and maintaining a pressure head on the scintillator in the containment vessel, is accomplished with a fluid handling system shown schematically in Fig. 1. In the initial filling, the shielding water tank (D200) and the scintillator containment vessel (D202) were filled simultaneously with high purity water maintaining the liquid levels in both to within 1 cm. An overpressure of 2 kPa of nitrogen was maintained inside the scintillator containment vessel during the filling operation to maintain the shape of the vessel.

The scintillator containment vessel was filled with scintillator by exchanging the water with scintillator. Water was incrementally drained from the bottom of D202 and subsequently replaced with scintillator. Scintillator from a 15 m^3 storage tank (D201), containing the scintillator inventory, was pumped by an all teflon reciprocating bellows pump through two 0.05 μm filters to a 0.5 m^3 ballast tank (D203) located on the top of the main water tank (D200). The liquid level in the ballast tank (D203) is set by an overflow tap with return to D201. Scintillator flowed to the scintillator containment vessel by gravity from the ballast tank. The ballast tank limits the hydrostatic pressure of the liquid delivered to the scintillator containment vessel (D202). This passive control system for the hydrostatic pressure is a fail safe system to control the pressure in the scintillator containment vessel, which in turn controls the shape of the flexible vessel. During the scintillator/water exchange the buoyant force on D202 increased causing the vessel to move upward as the strings restraining the vessel stretched. The vessel was continually repositioned using the winch and pulleys to keep it centered within the phototubes.

The fluid handling system was constructed entirely of stainless steel and teflon, with electropolished stainless steel employed wherever possible. The entire system was flushed with 3 M nitric acid, rinsed by copiously flowing deionized water and then dried with flowing nitrogen prior to use.

Pseudocumene (PC) for the scintillator was collected on-line at the production facility (Enichem, Sarroch, Sardinia) under a nitrogen atmosphere in clean 1 m^3 Teflon containers (Fluoroware), and immediately shipped to Gran Sasso and transferred to D201 to minimize cosmic ray exposure. Concentrated solutions of 200 g/l-PC were prepurified by water extraction, then added to D201 to achieve the desired final scintillator concentration of 1.5 g/l. The scintillator components in D201 were mixed by circulation of nitrogen gas through the scintillator in D201.

3.4. Scintillator purification system

Scintillator radiopurity requires removal of all forms of radioactive impurities that also exist as chemical impurities in the scintillator (^{3}H and ^{14}C are both radioactive impurities that cannot be removed from the scintillator). The chemical forms of these impurities are unknown, so purification methods were tested for the most likely impurities. The anticipated sources of radioactive impurities in the scintillator included: ^{222}Rn, ^{85}Kr and ^{39}Ar from air exposure; ^{238}U, ^{226}Ra and ^{232}Th from microscopic dust particles, and ^{40}K from the PPO. In addition ^{7}Be is produced cosmogenically from the ^{12}C(x, αxn)^{7}Be (x = n, p) reaction, and could contribute up to 1 Bq/kg to the background [37].

Preliminary laboratory tests of the optical properties and radiopurity of scintillator components and mixtures were studies after a variety of

purification processes [17]. These studies indicated that the scintillator solvent, pseudocumene, was radiopure of U, Th and K at the level $< 10^{-4}$ Bq/kg; the fluor, PPO, was also radiopure of U and Th at the level $< 10^{-4}$ Bq/kg. PPO, as purchased, was found to contain K contamination corresponding to 0.1 Bq/kg. The K was effectively removed by either vacuum distillation of the PPO or water extraction of concentrated solutions of PPO in pseudocumene. The optical properties of the scintillator were unaffected by water extraction. However, light transmission of the commercial sample of pseudocumene improved after distillation.

A purification system containing sub-micron filtration, water extraction, vacuum distillation, and nitrogen stripping was constructed to actively remove radioactive impurities. Filtration removes suspended dust particles larger than 0.05 μm. Water extraction is effective at removing ionizable species, such as metals (U, Th, K). Vacuum distillation removes low volatility components such as metals and dust particles. Nitrogen stripping removes dissolved gas impurities, such as ^{85}Kr, as well as water dissolved in the scintillator.

In normal operation, the scintillator is removed form the bottom of the scintillator containment vessel pumped through the purification system positioned on the top of the main water shielding tank (D200), and returned to the scintillator containment vessel. A schematic of the purification system is shown in Fig. 3. Scintillator is pumped through a countercurrent water extraction column, followed by a 0.05 μm filter. The scintillator, saturated with water, is passed countercurrently through a gas stripping column where water and dissolved gases are stripped by high purity nitrogen. Finally, the scintillator passes into a holding vessel which sets the pressure head in the scintillator containment vessel. In the alternate mode of operation the scintillator bypasses the water extraction system and is vacuum distilled in a falling film evaporator/condenser unit.

The purification system was constructed entirely of electropolished stainless steel, quartz and teflon. It was all cleaned in place with nitric acid rinses followed by copious flushing with high-purity deionized water. The plant capacity was 50 l/h in the water extraction mode and 20 l/h in the distillation mode. Details of the construction and operation of the purification plant are reported elsewhere [17].

3.5. *Water tank and clean room*

The tank containing the shielding water is constructed of 8 mm thick carbon steel, coated with

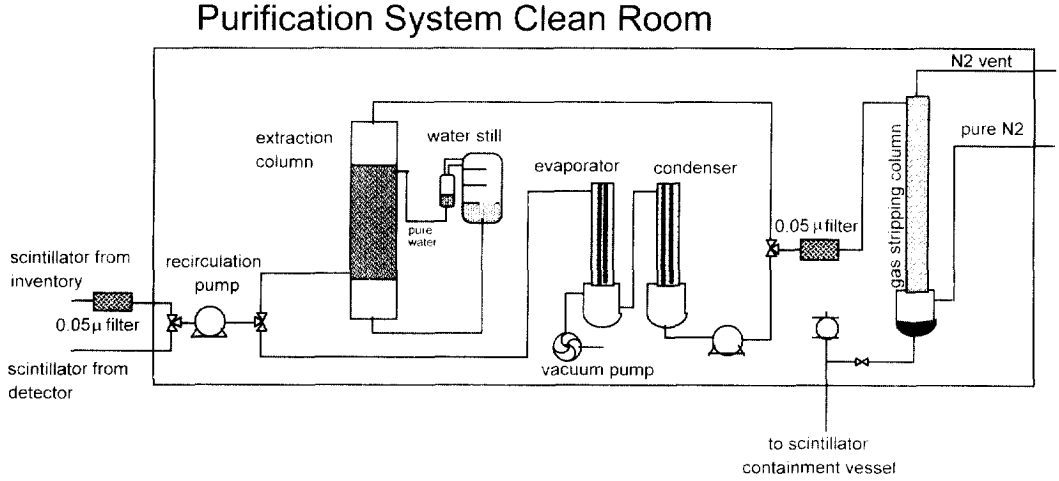

Fig. 3. Schematic of the scintillator purification system for CTF. The scintillator is either water extracted, or vacuum distilled then filtered and stripped with nitrogen before being returned to the scintillator containment vessel.

Permatex on the interior. It stands 10 m high and is 11 m in diameter. The scintillator containment vessel is centered horizontally, and vertically sits 4.5 m from the bottom of the water tank. A steel plate 5 m × 5 m × 50 mm thick was positioned below the center of the tank, to provide the equivalent of 4.5 m water shielding of the scintillator in all directions.

The principal access to the water tank is through 0.8 m × 1.5 m port. A class 100 clean room was constructed around this access port. During installation of the phototube support structure, phototubes, cabling and scintillator containment vessel, the air in the tank itself was filtered through HEPA filters maintaining the atmosphere in the tank as a class $< 10\,000$ clean room. All equipment installed in the main tank were wiped down and cleaned with deionized water in the clean room and then brought into the main tank for installation.

After installation the tank was sealed off and flushed with nitrogen. Water is pumped into the tank through a port 50 cm from the bottom of the tank. Water is removed from the water tank by overflow at a level 10 cm from the top of the tank. A nitrogen blanket is maintained over the top of the water in the water tank; an overpressure of 100 Pa is maintained, with a constant purge to sweep out radon. A Lucas cell continuously monitored the radon in the nitrogen blanket above the water. At the typical purge conditions the radon level in the nitrogen blanket is ~ 0.5 Bq/m^3.

3.6. The water purification system

Water is the main shielding of the active CTF volume; the design goal for radiopurity of the water is 10^{-6} Bq/kg. Water is purified through filtration, reverse osmosis, continuous deionization, ion exchange, and nitrogen stripping; a detailed description of the system is published [18,19].

The water purification system is shown schematically in Fig. 4. During the initial filling the plant operated in a production mode, in which raw water from the LNGS supply is purified. Water is first pre-filtered, passed through a reverse osmosis unit, and then deionized in a Continuous Deionization Unit (CDI). Before entering the water shielding tank the water is stripped of radon by countercurrent flow of nitrogen. The nitrogen stripping is critical as the LNGS water has a radon content of approximately 10^4 Bq/m^3.

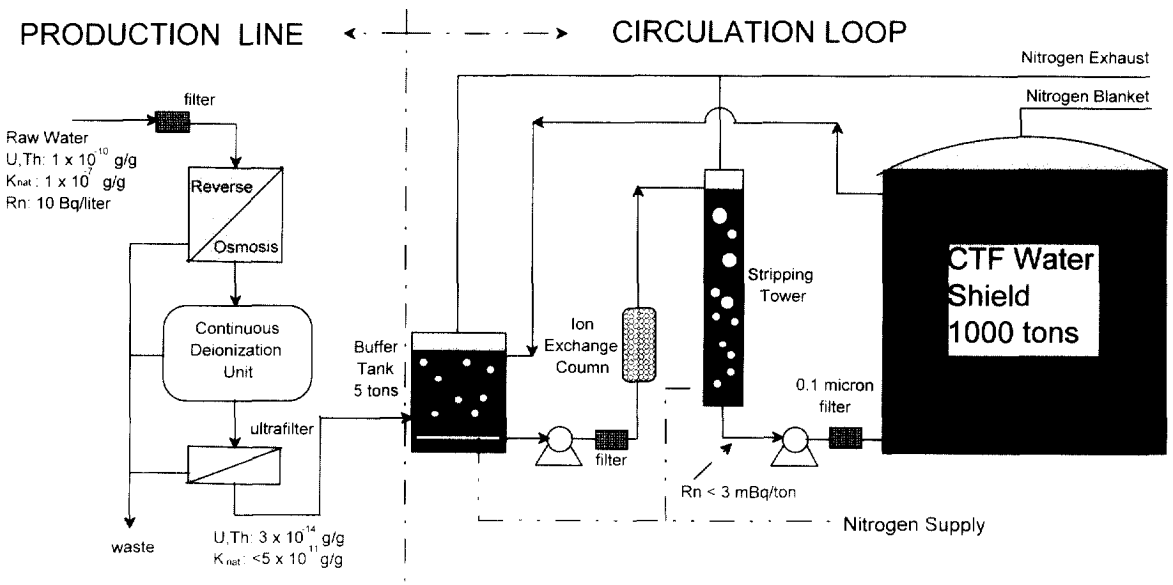

Fig. 4. Schematic of water purification system for the CTF.

After the initial filling the water is continuously repurified in a recirculation mode. Water is drawn off the overflow at the top of the water shielding tank and passed through a mixed (cationic and anionic) bed deionizer and the nitrogen stripping column and is then returned to the main water tank of the CTF. The CDI unit could not be used in the recirculation mode because it rejects 10% of the water in the deionization process, which would require fresh makeup water with higher radon content. The ion exchange beds have a limited exchange capacity which restricts their use to the recirculation mode where the water is prepurified.

The water system can purify 2 m^3/h of water in either the recirculation or production mode. The CDI unit reduces the ionic activity of the LNGS water from 10^{-10} g U,Th/g-water to 10^{-14} g U,Th/g water (10^{-13} g U,Th/g-water $\sim 10^{-6}$ Bq/m^3). The radon content in the water after nitrogen stripping with a nitrogen to water volumetric flow ratio of 10 is reduced to approximately 10 mBq/m^3.

The water system is constructed principally of PVC, and Teflon-coated steel.

3.7. *The photomultiplier system*

The scintillation light is detected by 100 0.20 m diameter photomulitplier tubes (Thorn EMI 9351). Detailed operating parameters of the phototubes and associated electronics are reported elsewhere [24–28]. In summary the tubes have a cathode efficiency of $\sim$25% (peak efficiency at 380 nm), transit time spread of 1 ns, dark noise of $\sim$500 Hz, low afterpulsing ($\sim$2.5%) and amplification of 10^7. The tubes are operated in the single photoelectron mode. The tubes were chosen especially for their low radioactivity, the bulbs are made of low radioactivity Schott 8246 glass. The components for the bases of the PMT were selected to minimize the radioactivity. The components in the base and the high-voltage line were sealed with a silicon gel to be resistant to water. The base assemblies were tested in water at a pressure of 0.1 MPa before installation. The dynodes of the PMT are shielded against magnetic fields with mu-metal collars. The final γ-ray activity of each tube assembly is $\sim$3.8 Bq.

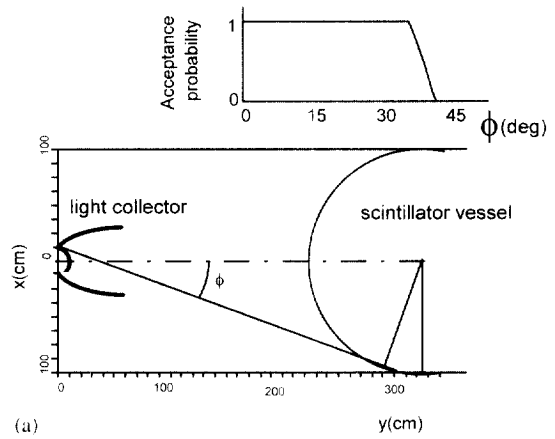

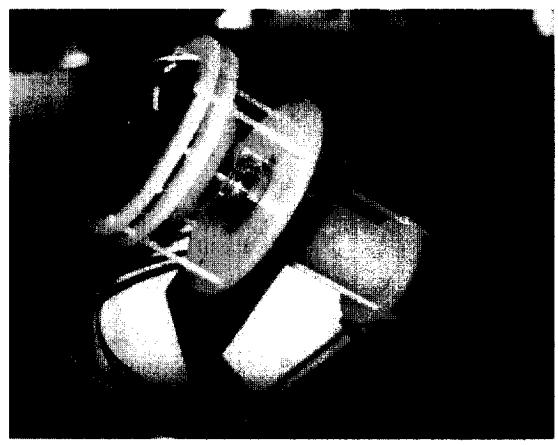
(b)

Fig. 5. (a) Schematic of Light Collectors for the CTF. The string cone geometry views the entire scintillator containment vessel, collecting the light and directing it to the photomultiplier. The collection efficieny drops off rapidly at angles beyond the scintillator vessel, as shown in the light transmission curve. (b) Photo of the assembly employed in the CTF. The light collector (not shown) is attached to the nylon support ring, the white plastic piece around the phototube.

The PMTs are a major source of background γ-rays. To shield the γ-rays background from the phototubes they are mounted 2.3 m away from the scintillator containment vessel. The PMTs are coupled to "truncated string cone" light concentrators [Welford and Winston], which collect the light from the scintillator containment vessel, but cut off the annular region between the vessel and the

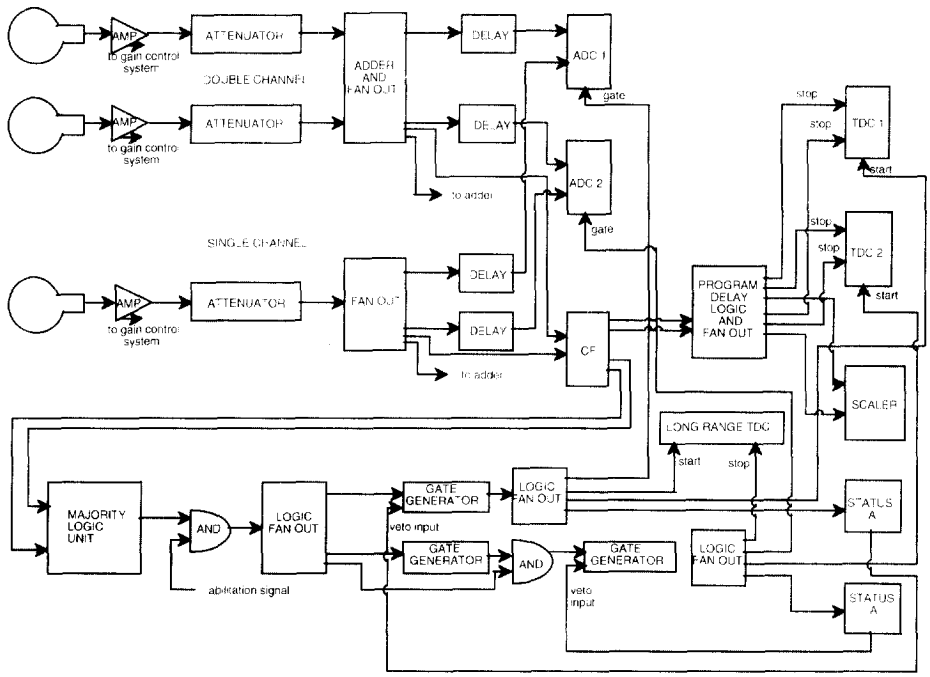

Fig. 6. Block diagram of the read-out electronics for the CTF.

phototubes (see Fig. 5). The light collectors preserve the area coverage of the active scintillator volume while moving the phototubes away. The geometrical coverage of the active scintillator region is 21%.

The light collectors were fabricated with low radioactivity UV-transparent acrylic with thin layers of silver and copper deposited on the outer surface of the acrylic. The metal layers were coated with an acrylic paint. The collectors are 57 cm long and have a 50 cm aperture. Details of the fabrication methods are provided elsewhere [30]. A photo of a completed light concentrator is shown in Fig. 5b.

Each PMT with the base, mu-metal shield and light concentrator was assembled as a unit and mounted on a stainless-steel ring structure inside the main water tank, as shown in Fig. 2. The phototubes were aligned during installation. A small laser was coupled to every light concentrator. The mounting bracket for the PMT assembly was adjusted so the laser light was directed at the nominal center of the ring structure, where the scintillator containment vessel would eventually be positioned. The accuracy of alignment was ~ 1–2 .

3.8. Data acquisition electronics

Every PMT assembly is equipped with a light guide which can be simultaneously triggered by a single laser pulse. Synchronizing on the rise time of the pulse permit the transmission times to be calibrated to an accuracy of 1.0 ns.

An independent control system on the high voltage maintained the photomultiplier gain. The dark noise single photoelectron peak is used in a feedback loop on most of the PMTs. A few PMTs display a broad noise pedestal, on those the high voltage is set from a special laser firing, where the laser intensity is set to have at most a single photoelectron detected.

Fig. 6 shows the data acquisition logic. The 100 photomultiplier outputs are processed in 64 electronics channels, 72 PMTs are fanned together in pairs into 36 channels and added together, and 28 PMTs are read as single channels. The output from

each channel is divided into an analog and digital signal. The analog signal passes into a pair of gated ADCs and to a linear adder which forms a 64-fold sum representing the total current, which is used for α–β discrimination. The analog signal is also passed through a constant fraction discriminator to a majority logic unit which generates an event trigger when it detects a threshold of PMT hits, typically 6 out of 100 within 30 ns (corresponding to a low-energy threshold of 25 keV).

When a trigger is generated a gate on the ADC is opened and a clock is started on TDCs for each channel. The ADC gate remains open for 500 ns charge integratson time. The total charge for an event is obtained integrating the 64-fold analog sum for 500 ns after the trigger. A long time "tail" is taken as the integrated charge beginning 32 ns after the trigger up to 500 ns. The ratio of the integrated charge in the tail to the total integrated charge is employed for α/β discrimination.

The TDC clock is stopped when a digital signal is detected in the corresponding channel. The intrinsic resolution of the electronic system is about 0.1 ns, evaluated via a start-stop sequence from an analog waveform generator. The event trigger also starts a separated TDC clock with a full scale of 8 ms. If a second event occurs within 8 ms it is processed through a second set of ADCs and TDCs, which permits analysis of event pairs that are correlated in time. These events are tagged as "group 2" events and principally arose from ^{214}Bi–^{214}Po decay sequence of radon daughters. Correlated events with delay times greater than 8 ms are measured directly with the internal clock of the computer.

A μVax CAMAC controlled data acquisition system loads the data from the ADCs and TDCs into a temporary buffer (with a capacity of $\sim$10 000 events) for on-line analyses. The data is then stored on Exabyte cassettes for retrieval. The data stored for each event include the total integrated charge for each channel, the time each channel is triggered, and the integrated charge for all channels along with the integrated charge for 32 500 ns.

3.9. Nitrogen system

Pure nitrogen is used as received from commercial vendors (SIO) as a blanket and for stripping radon from water. Liquid nitrogen is stored in a 10 m^3 cryogenic tank. As demanded the liquid is drawn into an evaporator, and heated to $\sim$20 C. The gaseous nitrogen is delivered from this plant at 4.5 bar; individual pressure regulators control the low pressure nitrogen in the blanket and the higher pressure nitrogen required for the water stripping column.

The radon content in the nitrogen used for stripping the scintillator must be below 10^{-7} Bq/m^3. A dedicated boil-off nitrogen draws from the main storage tank into a 3 m^3 tank. Vapor–liquid equilibrium at 4 bar is maintained in the 3 m^3 tank. Gaseous nitrogen is drawn from the top of this 3 m^3 tank. The vapor pressure of nitrogen at 90 K is approximately 10^6 greater than radon, so the vapor is depleted of radon relative to the liquid, insuring higher-purity nitrogen.

3.10. Ancillary facilities

A variety of the CTF functions are monitored with ancillary measurements. Conductivity, pH and temperature of the shielding water are continuously monitored at three locations within the water tank. Samples of the shielding water are removed and tested for radon. A preconcentration method followed by counting in a miniaturized low background gas counter achieved sensitivities of 1 mBq/m^3 [31]. Water samples were also tested for U and Th by inductively coupled mass spectroscopy [18], and neutron activation [38] with a sensitivity of 2×10^{-16} g U,Th/g-water.

Samples of scintillator are routinely checked for their optical attenuation length and fluorescence by spectrometers [20]. Measurements of U,Th and K in the scintillator were also obtained by high-sensitivity neutron activation analysis [38].

A muon telescope was installed on the top of the water tank to obtain unambiguous data on the CTF-response to muons. Two Ar–methane (90/10) multiwire proportional chambers (1.9 m $\times$ 1.8 m) independently detected muons entering the CTF. Pulse height distributions of Cherenkov events due to muons were correlated with muons detected by

the telescope. Details of the muon telescope and the results of the correlated measurements are reported elsewhere [39].

4. General performance of the CTF

The various parts of the CTF were installed during the period of 1993 – early 1995. The CTF was filled with water in January 1995, and the scintillator was put in during February–April 1995. The CTF ran continuously since it was filled with water in January of 1995 until July 1997.

4.1. Scintillator

A simple binary scintillator was chosen for the CTF. PPO was chosen as a single fluor based on its high quantum yield for fluorescence, price and availability, ease of purification, and the excellent match between its fluorescence spectrum and the phototube sensitivity. No diluent, such as mineral oil, was employed. Diluents complicate the purification of the scintillator, and do not significantly improve the light output.

The CTF detector calorimetrically measures the energy released during a scintillation event. The light output of the ^{214}Po α-decay (7.7 MeV) was corrected for the equivalent electron energy using the difference in light yield from α and γ excitation of the scintillator in separate laboratory experiments, giving a light yield for β and γ excitation of 300 ± 30 photoelectrons/MeV for 100 phototubes. The linearity of the detector was verified with the signals from ^{85}Kr, ^{222}Rn and ^{218}Po internal to the scintillator, and γ-lines from Rn decay in the shielding water. The energy scale of the CTF was recalibrated based on the ^{214}Po α-decay when phototubes failed. The energy resolution of the ^{214}Po α was 70 keV (1σ) with 100 phototubes. The energy resolution deteriorated with loss of phototubes, with the resolution scaling approximately as $n^{-1/2}$ (n being the number of phototubes). Details of the energy calibration are reported elsewhere [32].

The location of events in the CTF are reconstructed based on photon arrival times at the phototubes after the trigger. The probability density function of the photoelectron arrival times for the reconstruction is determined by mapping out events with known positions using a radon spiked scintillator source within the detector [39]. Details of event reconstruction are reported in detail elsewhere [32]. The spatial resolution of event reconstruction of the CTF detector is approximately 15 cm at 300 keV decreasing to 10 cm at 1 MeV, based on 100 phototubes.

Light scattering and reflections in the CTF was quantified using a window source, in which a shield limited the solid angle of the detector directly illuminated. Light arriving at the shielded phototubes revealed that 28% of the light is scattered over a distance of 1 m in the scintillator. The apparent decay time as measured by the cumulative detected charge in the CTF is lengthened to 4.5–5 ns due to both elastic and inelastic scattering processes.

4.2. Scintillator containment vessel

A novel aspect of the CTF detector is the use of a flexible vessel to contain the liquid scintillator. It proved to be superior to the more conventional rigid vessel design when the simultaneous constraints of transparency, tolerance of aromatic solvents, low radioactivity, and cost are considered. The flexible nylon vessel was made possible by the identification of optically clear amorphous nylons.

The vessel has sustained the buoyant force without irreversible deformation. A small amount of creep was observed in the nylon tether strings, which is easily compensated for by moving the hold-down plate. The nylon vessel showed no deterioration of the transparency over a period of two years in operation. To err on the side of safety the vessel was under inflated by 1–2%, which caused the vessel to distort slightly from spherical assuming a "balloon shape". The hold down strings on the vessel also created a small scalloping effect on the surface. Because of the optical mismatch between the scintillator and the water these shape distortions slightly complicate the positional reconstruction due to reflection and refraction at the water/vessel interface.

A problem unique to the thin membrane containment vessel is the diffusion of material through the membrane. Water will diffuse through the nylon until the pseudocumene becomes saturated

with water, at a concentration of ~100 ppm. The scintillator purification system removes the water by nitrogen stripping, which circumvents the problem of water phase separating out of solution in the case of decrease in the temperature of the scintillator.

Radon diffusion from the water through the nylon membrane into scintillator has been observed on several occasions when the radon concentration in the shielding water increased. Over time this resulted in a small increase in the long-lived radon decay products in the scintillator (i.e. ^{210}Pb, ^{210}Bi and ^{210}Po). The scintillator purification system removed these impurities. However, the permeability of the scintillator containment vessel to radon puts greater demands on the purity of the shielding water.

4.3. Scintillator purification system

On-line purification of the scintillator reduced the internal background rate in the CTF detector within the energy window of $250 < E < 800$ keV from ~470 events/day internal to the scintillator volume (events were selected by their reconstruction in space and energy) to < 40 events/day (85% confidence limit). The system is automated and ran under computer control with only minor operator input required. The nitrogen stripping is effective at reducing the water content in the scintillator and dissolved gases. In particular, a small amount of air exposure during the initial scintillator preparation and filling introduced ^{85}Kr into the scintillator, with a total event rate of 300 ± 100/d. Nitrogen stripping reduced the ^{85}Kr to below the limit of detection by the CTF.

Radon entered the scintillator during the preparation stages, and decayed away prior to the application of the purification procedures. The radon decayed to ^{210}Pb which accumulates as a result of its 22 yr half-life. The energy released by the decay of ^{210}Pb is below the threshold of the CTF, but ^{210}Po and ^{210}Bi, products of the decay of ^{210}Pb have sufficiently long lifetimes to accumulate in the scintillator, and the energies associated with their decay fall into the energy window of the CTF. ^{210}Po was identified in the CTF background based on the presence of an α-decay at the energy corresponding to ^{210}Po. Water extraction effectively reduced the ^{210}Po from ~200 events/day to < 40 events/day.

The purification system maintained the optical properties and radiopurity of the scintillator over the period of one year. The scintillator was stable; once high purity of the scintillator in the scintillator containment vessel was achieved, it was not necessary to continue to operate the purification system continuously.

The only problem encountered with the purification of the scintillator is the purity of the nitrogen used for nitrogen stripping. There is a source of radon in the system that limited the ultimate purity of the scintillator during nitrogen stripping operations to a radon event rate in the CTF of ~75 events/d. This level of radon was sufficiently low to allow it to decay away over a period of one month.

4.4. Water purification

The water plant for the shielding water maintained the resistivity of the shielding water at > 10 MΩ cm for both the recirculation mode and production mode of the water plant. ICP-MS and neutron activation analyses of the water demonstrated the U and Th levels were reduced to below 10^{-7} Bq/kg (from 10^{-3} Bq/kg in the raw LNGS water) and K was reduced from 2.5 Bq/kg to 5×10^{-3} Bq/kg. Radon in the water was reduced from 10 Bq/kg in the LNGS water to 5 μBq/kg after nitrogen stripping. The radon content of the shielding water internal to the main tank was inconsistent with the performance of the water purification system. The radon level of the shielding water is 30 μBq/kg. Spatial analysis of the scintillation events was consistent with this radon content in the water. Radon emanation from the Permatex coating of the water tank and leakage of air into the nitrogen blanket over the water are identified as potential sources of the radon in the shielding water. In addition dust in the tank, the photomultiplier tubes and bases and cables probably contribute to the radon in the tank as well.

4.5. Photomultiplier system

At some time after filling the CTF, 70 l of pseudocumene was found to be floating on top of

the shielding water buffer. This was not a leak from the scintillator containment vessel, and the source has never been identified. The pseudocumene attacked the silicone sealant on the bases of the photomultiplier assemblies permitting water to leak in and create an electrical breakdown. Over the 2 y of operation a significant fraction of the phototubes have stopped functioning which has degraded the quality of data from the CTF. Radiopurity measurements based on time-correlated events were not significantly affected by the loss of phototubes; however, spatial reconstrution, energy resolution, and α/β discrimination deteriorated with declining number of phototubes.

4.6. Signal discrimination

The sources of some of the events detected in the CTF can be identified by their specific signatures. The most effective signal discriminator is delayed time correlation of successive decay events along a decay chain. This method is applied to successive β and α decays in the uranium and thorium series, to a minor branch of ^{85}Kr where a γ-ray follows β-decay, and to γ-ray emission following neutron capture by hydrogen after its production from a cosmic muon. The properties of the decay sequences detected in the CTF are summarized in Table 1. The lower limit for time-correlated events is 100 ns, imposed by the detection electronics. The longest correlation time interval is determined by accidental coincidence of the correlation, which depends on the overall background rate. This background can be reduced by selecting events with the proper energy, spatial position, and where applicable the proper particle discriminator. In practice, this procedure is inverted; the time correlation is used to select the energy of the ^{214}Po α-particles, which calibrate the energy and position of events.

Cosmic muons are a major source of events in the CTF. Nearly, 75% of the muon-induced events produce light output corresponding to energies of >1 MeV, which are outside the energy window of interest. Muon induced events with energy <1 MeV arise from Cherenkov light produced in the shielding water. Part of the Cherenkov light from the water is seen directly by the phototubes, the UV Cherenkov light also excites the scintillator which fluoresces. Many of these events may be discriminated from low-energy events in the scintillator because the Cherenkov light is produced over a large region, and causes a considerable time spread in the signal arriving at the phototubes. The mean arrival time of the photoelectrons was >16 ns. The efficiency for muon identification that passed through the water was improved by using the up/down asymmetry for photon detection. The Cherenkov light is directed down giving rise to more charge detected in the phototubes in the lower hemisphere of the CTF detector. Application of both the timing cut and the spatial asymmetry gave an efficiency of muon rejection of 95%, while retaining $>95\%$ of the scintillation events. The efficiency of the muon detection was tested by selecting muons with two external wire chamber in coincidence with their detection in the scintillator and measuring their event time distribution in the scintillator.

Table 1

Decay sequence	Mean lifetime	Source
^{214}Bi(β)–^{214}Po(α)	236 μs	^{238}U
^{212}Bi($\beta+\gamma$)–^{212}Po(α)	432 ns	^{232}Th
^{85}Kr(β)–^{85}Rb(γ)	1 μs	^{85}Kr
>1 MeV (muon)-n-2.2 MeV γ	269 μs	Cosmic muon

A second class of events were observed in the CTF that also showed the long mean arrival time, but these events showed more charge collected in the upper hemisphere of the detector. Between 100–200 events/day were detected with this time and spatial distribution. These events were not associated with scintillation as they were also observed when the scintillator containment vessel was filled with water. The source of these events is presently unknown. Their signature is very distinct from scintillation events and they can be efficiently identified, and a cut applied to remove them from the background.

Scintillation generated by α events are distinguished from β and γ events by the event decay time, where the fraction of the photocurrent

collected from 32 to 500 ns to the photocurrent collected from the trigger to 500 ns was used as the discriminator. The α/β discrimination was examined in the CTF utilizing the ^{214}Bi–^{214}Po decay signals. With 100 phototubes $> 90\%$ of the 7.7 MeV ^{214}Po(α) were identified with less than 5% β-events misidentified as an α-event (the efficiency of α/β discrimination is improved significantly when the discriminator is optimized for spatial position of the event [32]). As the number of phototubes decreased the α/β discrimination deteriorated.

5. Radiopurity measurements

A principal goal of the CTF was to test the intrinsic radiopurity of liquid scintillators, as a basis for low background detectors. The primary results of the measurements with the pseudocumene/PPO scintillator are highlighted below, the details of the radiopurity of the scintillator are provided elsewhere [32].

After pre-purifying the PPO by water extraction from concentrated solutions, and employing the pseudocumene as received from the factory the total internal background rate was 470 ± 90 events/d (this is the total event rate or singles rate internal to the scintillator). ^{85}Kr from exposure of the scintillator to ~ 4 l of air accounted for 300 ± 45 events/d. 250 ± 40 events/d have been tentantively identified with the decay of ^{210}Po that accumulated from the decay of ^{222}Rn. (Events from ^{210}Bi are expected in the energy window of interest, but the β-decay from ^{210}Bi does not have a monoenergetic signature to identify its presence.) Nitrogen stripping successfully removed the ^{85}Kr. Water extraction removed the ^{210}Po impurity. After purification the internal radioactive background in the scintillator was reduced to < 40 events d. The spatial distribution events suggests there are ~ 170 events/d from the surface of the scintillator containment vessel after purification. Radium (uranium) and thorium concentrations in the scintillator, inferred from maximum likelihood analyses of the $\beta\gamma/\alpha$ delayed coincidences of the Bi Po decays of the respective chains, are Ra(U) = 4×10^{-9} Bq/kg and Th $< 10^{-9}$ Bq/kg, respectively.

The ^{14}C contamination in the scintillator was determined from the spectrum shape in the 60–100 keV range to be $\sim 3 \times 10^{4}$ Bq/kg (isotopic abundance $^{14}C/^{12}C \sim 2 \times 10^{-18}$) [33].

The ^{14}C, U and Th radiopurity of the scintillator remained stable for over a year. After purification the ^{85}Kr and ^{210}Po did not reappear, and the low intrinsic background of the scintillator was stable for several months.

6. Conclusions

The counting test facility demonstrated the feasibility of a large-scale low background liquid scintillation detector. Confinement of the liquid scintillator within a water shield by a flexible nylon vessel is a new technology for large-scale detectors. On-line purification of a liquid scintillator achieved radiopurity levels below detection and maintained the optical properties of the scintillator.

Radiopurity of a liquid scintillator at the level of $\sim 10^{-9}$ Bq/kg above 250 keV, and $\sim 10^{-3}$ Bq/kg below 250 keV has beendemonstrated in the CTF. This purity is promising for the feasibility of utilizing a liquid scintillation detector for Solar Neutrino detection.

Acknowledgements

Funding for the Counting Test Facility was provided by the Italian Institute for Nuclear Physics (I.N.F.N.), the Deutsche Forschungsgemeinschaft (DFG), SFB 375-Astro Particle Physics, and the Tandem Accellerator TU/LMU Muenchen and the United States National Science Foundation (PHY-9313919).

References

[1] J.N. Bahcall, Neutrino Astrophysics, Cambridge University Press, Cambridge, England, 1989.
[2] D.N. Schramm, S.E. Woosley (Eds.), Nuclear Astrophysics: Proc. Caltech Centennial Year Nuclear Astrophysics Symposium in Honor of William A. Fowler's 80th birthday, Phys. Rep. 227 (1–5) (1993).
[3] J.N. Bahcall, Astrophys. J. 467 (1996) 475.

[4] M. Koshiba, Phys. Rep. 220 (5–6) (1992).
[5] D.N. Schramm, J.W. Truran, Phys. Rep. 189 (2) (1990).
[6] T. Gaisser, F Halzen, T. Stanev, Phys. Rep. 258 (3) (1995).
[7] P.F. Smith, J.D. Lewin, Phys. Rep. 187 (5) (1990).
[8] G. Jungman, M. Kamionkowski, K. Griest, Phys. Rep. 267 (5–6) (1996).
[9] R. Barloutand, Nucl. Phys. B (Proc. Suppl.) 28A (1992) 437.
[10] M.S. Turner, E.N. Parker, T.J. Bogdan, Phys. Rev. D 26 (1982) 1296.
[11] MACRO Collaboration, M. Ambrosio et al., Astroparticle Phys. 6 (1996) 113.
[12] Y. Suzuki, Nucl. Phys. B. (Proc. Suppl.) 38 (1995) 54 [Neutrino '94]
[13] G. Aardsma et al., Phys. Lett. B 194 (1987) 321.
[14] V. Beresnev et al., Proc. 16th Int. Cosmic Ray Conf., University of Tokyo, Tokyo, vol. 10, 1979, p. 293.
[15] Borexino at Gran Sasso, Proposal for a real time detector for low energy solar neutrinos, I.N.F.N., August 1991; A real time detector for low energy solar neutrinos, Princeton University, December 1992.
[16] J.B. Benziger, F.P. Calaprice, M. Chen, N. Darnton, M. Johnson, F. Loeser, R.B. Vogelaar, A flexible confinement system for a large scale low background scintillation detector, in preparation.
[17] J.B. Benziger, F.P. Calaprice, M. Chen, N. Darnton, M. Johnson, F. Loeser, R.B. Vogelaar, A purification system for a large scale low background detector, in preparation.
[18] M. Balata, L. Cadonati, M. Laubenstein, G. Heusser, M. Giammarchi, R. Scardaoni, V. Torri, G. Cecchet, A. de Bari, A. Perotti, Nucl. Instr. and Meth. A 370 (1996) 605.
[19] M.G. Giammarchi, M. Balata, R. Scardaoni, Ultrapure Water J. 13 (1995) 59.
[20] F. Masetti, F. Elisei, U. Mazzucato, J. Lumin. 68 (1996) 15.
[21] F. Gatti, G. Morelli, G. Testera, S. Vitale, Nucl. Instr. and Meth. A 370 (1996) 609.
[22] G. Ranucci, Nucl. Instr. and Meth. A 354 (1995) 389.
[23] G. Ranucci, A. Preda, Nucl. Instr. and Meth. A 370 (1995) 597.
[24] G. Ranucci, R. Cavaletti, P. Inzani, I. Manno, Nucl. Instr. and Meth A 324 (1993) 580.
[25] G. Ranucci, M. Campanella, R. Cavaletti, D. Giugni, S. Magni, A. Preda, I. Manno, P. Ullucci, Nucl. Instr. and Meth. A 333 (1993) 553.
[26] G. Ranucci, S. Bonetti, R. cavaletti, I. Manno, P. Ullucci, S. Schoenert, Nucl. Instr. and Meth. A 330 (1993) 276.
[27] G. Ranucci, Nucl. Instr. and Meth. A 335 (1993) 121.
[28] G. Ranucci, D. Giugni, I. Manno, A. Preda, P. Ullucci, A. Golubchikov, O. Smirnov, Nucl. Instr. and Meth A 337 (1993) 211.
[29] G. Ranucci, P. Ullucci, S. Bonetti, I. Manno, E. Meroni, A. Preda, Nucl. Instr. and Meth. A 350 (1994) 338.
[30] J.X. Prochaska, The design and fabrication of optimal light collectors for the CTF upgrade, Thesis, Princeton University, 1993.
[31] M. Laubenstein et al., High sensitivity measurements of radon, in preparation
[32] Borexino Collaboration, Ultra-low ground measurements in a large volume underground experiment, Astroparticle Phys., submitted.
[33] Borexino Collaboration, Measurement of the 14C abundance in a low-background liquid scintillator, Phys. Lett. B, submitted.
[34] J.B. Birks, The Theory and Practice of Scintillation Counting, Macmillan, New York, 1964.
[35] C.-T. Peng, D.L. Horrocks, E.L. Alpen (Eds.), Liquid Scintillation Counting: Recent Applications and Development, Academic Press, New York, 1980.
[36] Borexino Collaboration, light propagation in large-scale liquid scintillator detectors, in preparation.
[37] R.B. Vogelaar, J. Benziger, F.P. Calaprice, N. Darnton, Nucl. Instr. and Meth. A 372 (1996) 59.
[38] T. Goldbrunner, J. Radioanalyt. and Nucl. Chem. 216 (2) (1997) 293.
[39] T. Hagner, C. Hagner, L. Oberaurer, Muon detection in the counting test facilty, to be published.